JOURNAL OF MARINE SCIENCES & ENVIRONMENTAL TECHNOLOGIES
Vol. 7, Issue No. 2 (December-2021)

ISSN (Print): 2413-5267
ISSN (Online): 2706-9966

TEM Image Analysis of Fracture Surfaces of P91 Steel and Comparison with Mechanical Properties

Abubkr Mohamed Hemer[1], L.J. Milovic[2], Muammar M. Ben Isa[3, *], and Abdusalam M. Sharf[3]

[1)] Higher Institute of Engineering Technology, Zliten, Libya.
[2)] Faculty of Technology and Metallurgy, University of Belgrade, Karnegijeva 4, 11120 Belgrade, Serbia.
[3)] Faculty of Engineering, Alasmarya Islamic University, Zliten, Libya.

[*]**E-mail:** m.benisa@asmarya.edu.ly

تحليل صور TEM لأسطح الكسر لصلب P91 ومقارنتها بالخواص الميكانيكية

أبوبكر محمد حمير[1]، ميلوفيتش[2]، معمر بن عيسى[3، *]، عبدالسلام شرف[3]

[1)] المعهد العالي للتقنيات الهندسية، زليتن، ليبيا.
[2)] كلية التكنولوجيا والمعادن، جامعة بلغراد، كارنيجيفا 4 ، 11120 بلغراد ، صربيا.
[3)] كلية الهندسة، الجامعة الأسمرية الإسلامية، زليتن، ليبيا.

Received: 28 November 2021; Revised: 06 December 2021; Accepted: 10 December 2021.

Abstract

In order to improve the efficiency of steam boilers in modern power plants, engineers have to use contemporary materials that enable exploitation at higher parameters, primarily operating temperature and pressure, with resistance to different forms of corrosion at the same time. For that purpose, contemporary 9-12Cr martensitic steels, designated P91, P92, E911, VM12-SHC, and SHM12, were developed.

The paper analyzes experimental research on the behavior of commercial ferritic steel P91 samples. Behavior data on the heat affect zone (HAZ) of welded joints were obtained by testing smooth specimens produced by simulation of the new material welding. A survey of testing hardness and tensile properties is given and images of the fracture surfaces of the samples were processed. Image analysis with ImagePro Plus confirmed experimental testing results for the grain size measured by the circle method and a comparative relationship between the percentage of carbides, precipitates, and lamellar diameters with respect to temperature is provided. The material that was PWHT (post-weld heat treatment) has the highest mean value of lamellar diameter, which indicates increased toughness and decreased hardness compared to BM and material without PWHT i.e (The higher lamellar diameter, the smaller material hardness).

***Keywords**: Images analysis, Thermal simulation, P91, PWHT, ImagePro Plus software.*

الملخص

من أجل تحسين كفاءة الغلايات البخارية في محطات الطاقة الحديثة، يتعين على المهندسين استخدام المواد المعاصرة التي تتيح استغلال معايير أعلى، بشكل أساسي درجة حرارة والضغط التشغيليين، مع مقاومة أشكال مختلفة من التآكل في نفس الوقت. لهذا الغرض، تم تطوير الفولاذ المارتنسيتي المعاصر 9-Cr12، والتي تسمي أو يرمز لها حديثاً بـ P91، P92، E911، VM12-SHC و SHM12.

تحلل الورقة البحث التجريبي على سلوك عينات الصلب الفريتي التجاري P91. تم الحصول على بيانات السلوك على منطقة التأثير الحراري (HAZ) للوصلات الملحومة عن طريق اختبار العينات الناعمة الناتجة عن محاكاة مادة اللحام الجديدة. تم إجراء مسح لاختبار الصلابة وخصائص الشد ومعالجة

ISSN (Print): 2413-5267
ISSN (Online): 2706-9966

صور لأسطح الكسر في العينات. أكد تحليل الصورة باستخدام ImagePro Plus نتائج الاختبارات التجريبية لحجم الحبيبات المقاسة بطريقة الدائرة وتم إيجاد علاقة مقارنة بين النسبة المئوية للكربيدات والرواسب والأقطار الصفائحية فيما يتعلق بدرجة الحرارة. تحتوي المادة التي كان لها PWHT (المعالجة الحرارية اللاحقة للحام) على أعلى متوسط لقطر الصفائح، مما يشير إلى زيادة المتانة وانخفاض الصلابة مقارنةً بالمعدن الأساسي (BM) والمواد التي بدون PWHT أي أن (كلما كان القطر الرقائقي أعلى، كانت صلابة المادة أصغر).

الكلمات الدالة: تحليل الصور، المحاكاه الحرارية، P91، PWHT، برنامج أمج برو أبلس.

1. Introduction

Thermodynamic efficiency of steam turbine in electricity production in fossil fuel power plants can be increased if temperature and steam pressure are increased at turbine inlet. That is why steels operating under harder conditions are developed to meet the requirements of efficient electricity production.

The material used in this work is commercial ferritic steel P91 that is used for manufacturing the process equipment components in fossil fuel power plants operating under supercritical steam conditions (steam temperature 600 ºC and steam pressure up to 290 bar). Testing involved the behavior of welded joints of the steam line components manufactured of the material P91. Behavior data on HAZ of welded joints were obtained by testing smooth specimens produced by simulation of the new material welding (Pandey *et al*., 2018; Burzić *et al*., 2008; Burzić & Adamović, 2008; and Shibli & Hamata, 2001). The paper presents the results of testing hardness and tensile properties, carried out in previous research, as well as the processing of images of the samples' fracture surfaces. Measured lamellar diameters, percentage of carbides and precipitates were compared depending on whether or not additional heat treatment has been done, and conclusion was drawn on material hardness. Also, comparison was made between the grain size measured by the circle method and the grain size measured using ImagePro Plus program.

2. Experimental

Using the Gleeble system to simulate of the heat-affected zone, thermal fatigue, many other metallurgical studies and the test hot ductility properties. Samples are placed between two sets of jaws that are part of a high current circuit. As current passes through the sample, it is resistively heated. A thermocouple welded to the center of the sample is used in a feedback loop to monitor temperature and control current (Nippes and Savage, 1949). A sketch of the jaws, sample, and thermocouple wires is shown in Figure (1).

The data on behaviour of the heat-affected zone (HAZ) of the welded joints were obtained by testing of smooth specimens made by simulation of welding of new material. The aim of performed experiment was to determine hardness values and tensile properties of the sample of base metal, designated BM in this work, and two samples simulated at maximum temperature of 925 ºC, so as to obtain the microstructure of characteristic HAZ. After simulation of the welding process, one sample was subjected to additional heat treatment and

ISSN (Print): 2413-5267
ISSN (Online): 2706-9966

designated 925 ºC with PWHT. Another sample that has not been subjected to additonal heat treatment was designated 925 ºC without PWHT.

Figure 1. Specimen thermocouples welded at center after thermal simulation

2.1. Material

The base material 9% Cr steel designated X10CrMoVNb 91 (P91) is martensitic steel microalloyed with vanadium, niobium and nitrogen (Milović *et al*., 2013; Vuherer *et al*., 2013; Milović , 2010; and Milović *et al*., 2008).

Testing was conducted on a pipe Ø320 mm, wall thickness 14 mm, which ensures conditions of plane stress state during testing, length 140 mm, manufactured of steel whose chemical composition, Table (1), was determined at the Laboratory for quality assurance, US Steel Serbia.

Table 1. Chemical composition of tested material (weight %)

C	Si	Mn	P	S	Cu	Al	Cr	Mo
0.120	0.289	0.396	0.009	0.002	0.082	0.024	8.04	0.850

2.2. Mechanical properties

The tensile test method provided information on mechanical properties of the tested metal. Material hardness and tensile properties were tested according to standard code.

2.2.1. Testing hardness

Hardness value measured at 600 ºC on the BM sample, 925 ºC without PWHT and 925 ºC with PWHT are presented in Table (2).

Table 2. BM hardness and simulated samples 925ºC with and without PWHT

Tested material	Hardness
BM	230 HV1
HAZ 925ºC without PWHT	380 HV5
HAZ 925ºC with PWHT	205 HV10

Measured hardness values are within the limits prescribed according to WGB 508L for the material designated X10CrMoVNb91. Hardness is noticed to decrease in the material subjected to post heat treatment.

ISSN (Print): 2413-5267
ISSN (Online): 2706-9966

2.2.2. Tensile properties

Table (3) shows tensile properties of all three samples at operating temperature (ISO E., 2012).

Table 3. Tensile properties of tested material

Tested material	Temperature of testing [ºC]	Tensile strength R_m [MPa]	Yield stress $R_{p0,2}$ [MPa]
BM	600	313.5	231
HAZ 925ºC without PWHT	600	498	407
HAZ 925ºC with PWHT	600	363	295

Figure (2) shows the obtained corresponding diagrams in the stress-deformation system. We note from the stress and elongation curve between the base metal and the tested samples. The highest value of the tensile stress and yield point at without PWHT sample while it is lower at the PWHT.

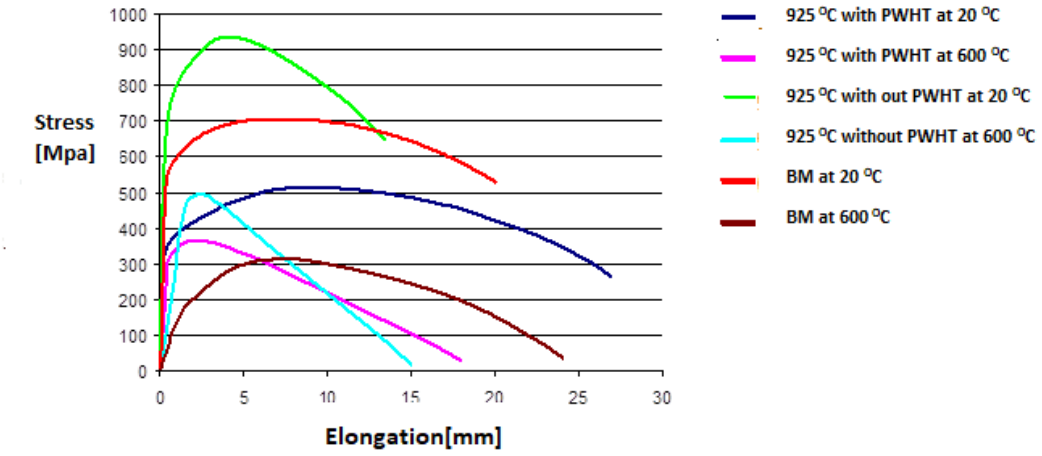

Figure 2. Comparison of BM tensile properties and tested samples at operating temperture

Also from Figure (2), we are observing an increase in elongation with stress constant, *i.e.* the material is not subject to Hook's law, F(x)=K(x) the material cannot recover its original shape after force is removed from it.

3. Image Analysis

The samples of characteristic states 925 ºC with PWHT, 925 ºC without PWHT and BM were prepared for transmission microscopy, then imaged and analyzed at the Laboratory for transmission electron microscopy, Belgrade University, Faculty of Technology and Metallurgy.

ISSN (Print): 2413-5267
ISSN (Online): 2706-9966

The obtained images were subjected to analysis in ImagePro Plus program (Vuksanović et al., 2018; Sun & Liao, 2016; and Liang et al., 2015). The microstructure of base material is shown in Figure (3).

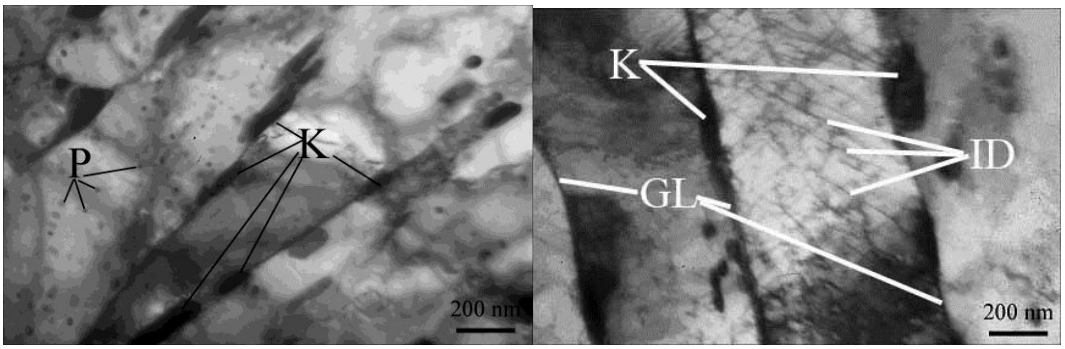

(a) *(b)*

Figure 3. Micostucture of structure of the base material. P= precipitates, K= carbides, ID= individual dislocations, & GL=Grain line

The base material consists of lamellar martensite with separated elongated carbides along the borders of the lamellae. The lamellar borders are clearly marked, which indicates that there is no strain on the borders. Besides elongated carbides, triangular carbides were noted, as well as the presence of precipitates along the lamellar borders, Figure (3b). Inside of the lamellae, separated precipitates are present as well. Generally, the base material has individual dislocations, does not have stress on the grain boundary, and the width of the lamellae can be easily measured.

ImagePro Plus program was used to measure the value of the lamellar diameters and percentage of carbides and precipitates. Table (4) displays values obtained by measurements, and graphic representation of the percentage of carbides and precipitates, Figures (4 & 5).

Table 4. Mean values of the lamellar diameters, percentage of carbides and precipitates

Tested material	Mean value of lamellar diameters [nm]	Mean value of carbides percentage [%]	Mean value of precipitates percentage [%]
BM	426.9356	5.1824	2.7390
925 ºC without PWHT	388.3474	1.4528	0.3505
925 ºC with PWHT	548.6977	2.8081	0.3786

ISSN (Print): 2413-5267
ISSN (Online): 2706-9966

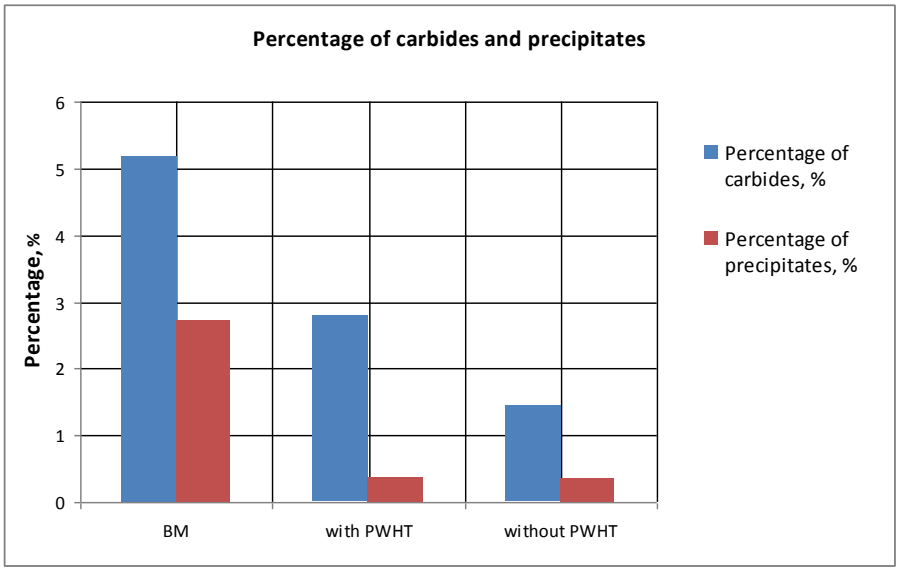

Figure 4. Percentage of carbides and precipitates.

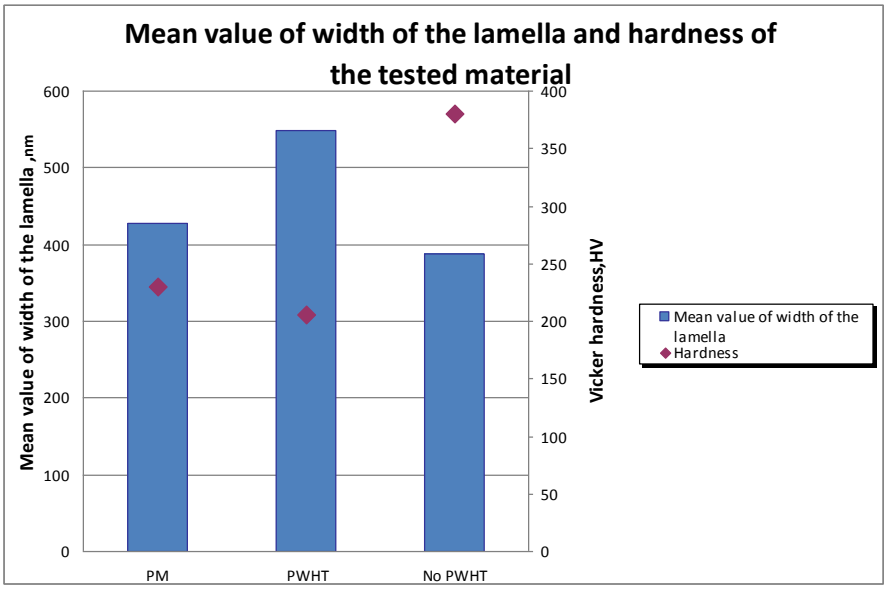

Figure 5. Mean value of width of the lamella and hardness of the tested material.

ImagePro Plus software was also used to measure the grain size and it was compared with the manual grain size measuring method, based on the circle method "Metallography", Schumann. Table (5) shows mean grain size after ASTM E112 "Standard Test Methods for Determining Average Grain Size" (ASTM E112), mean grain size measured by the manual circle method and mean grain size measured using ImagePro Plus program for digital analysis. Comparative relationship between these two methods is also presented in Figure (6).

ISSN (Print): 2413-5267
ISSN (Online): 2706-9966

Table 5. Grain size measurements in ImagePro Plus program

Simulated temperature zone T_p [°C]	Mean grain size after ASTM	ImagePro Plus Mean grain diameter [μm]	Manual circle method, Mean grain diameter [μm]
Initial structure BM	6.5	34.13	37.8
850	8	22.4	22.5
900	9.5	12.99	13.3
925	12	7.79	5.6
950	11	9.26	7.9
1000	10.5	12.07	9.4
1150	10.5	18.98	18.9
1200	10	32.18	31.8
1300	9.5	37.97	37.8
1386	9	54.38	53.4

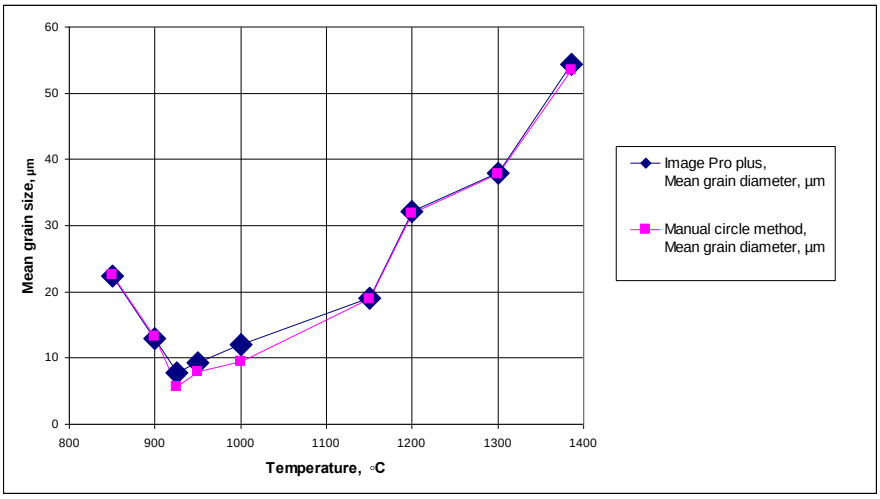

Figure 6. Graphic representation of comparative relationship between grain sizes measured by different methods

4. Discussion

When testing to get mechanical properties, a reduction in the hardness of the material post heat treated is noticeable. It is evident from Figure (2) that additional heat treatment has increased the capacity of plastic deformation prior to fracture. Also, by additional heat treatment for HAZ, the tensile properties approached tensile properties of the base material.

It can be seen in Table (4) and Figure (5) that mean value of lamellar diameter is the highest for the case of the sample 925 ºC with PWHT, then successively decreases for BM and 925ºC without PWHT. Also, mean value of carbides and precipitates percentage, Figure (4) is lower for the sample without PWHT than for the sample with PWHT. It can be also noted that hardness value is the lowest for the case of the highest lamellar width.

In grain size measurements the deviations are very small, Figure (6) therefore it can be concluded that ImagePro Plus method applied for tested samples confirms the results obtained

ISSN (Print): 2413-5267
ISSN (Online): 2706-9966

by standard laboratory method, which evidences that such method can be used for the analysis of steel microstructure characteristics.

5. Conclusion

The presented experimental results indicate the necessity for application of post weld heat treatment (PWHT) on each welded joint of highly loaded part of the steam line that is installed in the components in fossil fuel power plants, because:

- In samples of the same material post heat treated (after welding), hardness is smaller compared to the sample without additional heat treatment.
- Tensile properties indicate that the material post heat treated has higher toughness compared to the material without post heat treatment.

Image analysis leads to the following conclusions:

- The material that was post heat treated has the highest mean value of lamellar diameter, which indicates increased toughness and decreased hardness compared to BM and material without PWHT. (The higher lamellar diameter, the smaller material hardness).
- Also, the percentage of carbides and precipitates is higher in the sample with PWHT than in the sample without PWHT, which leads to the conclusion that carbides have positive effects on material toughness.
- By increasing the percentage of carbides and precipitates, the hardness decreases but toughness increases.
- ImagePro Plus method can be applied for the analysis of steel microstructure characteristics.

Acknowledgements

This work is a contribution to the Ministry of Education and Science of the Republic of Serbia funded Project TR 35011.

References

ASTM E112. *Standard Test Methods for Determining Average Grain Size*. Available online at: [https://tubingchina.com/ASTM-E112.pdf].

Burzić M. & Adamović Z. (2008). Experimental Analysis Of Crack Initiation And Growth In Welded Joint of Steel For Elevated Temperature. *Materiali in Tehnologije*, 42(6): 263-271.

Burzić M., Prokic-Cvetkovic R., Grujic B., Atanasovska I., & Adamović Z. (2008). Safe Operation of Welded Structure with Cracks at Elevated Temperature. *Strojniski Vestnik-Journal of Mechanical Engineering*, 54(11): 807-816.

ISO E. (2012). 6892-1. *Metallic materials-Tensile testing-Part 1: Method of test at room temperature*. International Organization for Standardization.

ISSN (Print): 2413-5267
ISSN (Online): 2706-9966

Milović L. (2010). Microstructural investigations of the simulated heat affected zone of the creep resistant steel P91. *Materials at High Temperatures*, 27(3): 233-242.

Milović L., Vuherer T., Blačić I., Vrhovac M., & Stanković M. (2013). Microstructures and mechanical properties of creep resistant steel for application at elevated temperatures. *Materials & Design*, 46: 660-667.

Milović L., Vuherer T., Zrilić M., Sedmak A., & Putić S. (2008). Study of the simulated heat affected zone of creep resistant 9–12% advanced chromium steel. *Materials and Manufacturing Processes*, 23(6): 597-602.

Nippes E.F. & Savage W.F. (1949). Development of specimen simulating weld heat-affected zones. *Welding journal*, 28(11): 534-546.

Pandey C., Mahapatra M.M., Kumar P., & Saini N. (2018). Some studies on P91 steel and their weldments. *Journal of Alloys and Compounds*, 743: 332-364.

Shibli I.A. & Hamata N.L.M. (2001). Creep crack growth in P22 and P91 welds—overview from SOTA and HIDA projects. *International journal of pressure vessels and piping*, 78(11-12): 785-793.

Sun Q. & Liao Y. (2006). Microstructure, Properties and Image-Pro Plus Analysis on Carburizing Austenitic Stainless Steel. *Foundry Technology*, 37(3): 445-447.

Vuherer T., Dunđer M., Milović L.J., Zrilić M., & Samardžić I. (2013). Microstructural investigation of the heat-affected zone of simulated welded joint of P91 steel. *Metalurgija*, 52(3): 317-320.

Vuksanović M.M., Gajić-Kvaščev M., Dojčinović M., Husović T.V., & Heinemann R.J. (2018). New surface characterization tools for alumina based refractory material exposed to cavitation-Image analysis and pattern recognition approach. *Materials Characterization*, 144: 113-119.

Zhao L., Liu W.L., & Ying W. (2015). Application of Image-Pro Plus in the groove filter rod characteristic parameters measurement. In: *Applied Mechanics and Materials*, 742: 111-117.